MEIS Investigations of Surface Structure

D.P. Woodruff*

Physics Department, University of Warwick, Coventry, UK

Abstract

The early work of the FOM-AMOLF group in Amsterdam clearly demonstrated the potential of MEIS (medium energy ion scattering), typically using 100 keV H^+ incident ions, to investigate the structure of surfaces, but most current applications of the method are focussed on near-surface compositional studies of non-crystalline films. However, the key strengths of the MEIS technique, notably the use of blocking curves in double-alignment experiments, and absolute yield measurements, are extremely effective in providing detailed near-surface structural information for of the a wide range of crystalline materials. This potential, and the underlying methodology, is illustrated through examples of applications to the study of layer-dependent composition and structure in alloy surfaces, in studies of the surface crystallography of an oxide surface (rutile TiO_2(110)) and in investigations of complex adsorbate-induced reconstruction of metal surfaces, including the pseudo-(100) reconstruction of Cu(111) induced by adsorption of atomic N and molecular methyl thiolate (CH_3S-). In addition to the use of calibrated blocking curves, the use of the detailed spectral shape of the surface peak in the scattered ion energy spectra, as a means of providing single-atomic layer resolution of the surface structure, is also discussed.

PACS: 68.49.Sf; 61.85.+p; 68.35.Bs; 68.35.Dv; 68.43.Fg; 68.47.Gh

Keywords: surface structure; surface reconstruction; MEIS; ion scattering; oxide surfaces; surface segregation; surface adsorption

* email@ d.p.woodruff@warwick.ac.uk

1. Introduction

Medium energy ion scattering (MEIS) [1] is closely related to the standard method of materials analysis of Rutherford backscattering (RBS), but the use of somewhat lower energies (typically ~100 keV rather than ~1 MeV) H^+ or He^+ incident ions allows one to achieve significantly higher depth resolution and to exploit more fully the potential to extract near-surface crystallographic information. The development of MEIS can be largely attributed to work at the FOM AMOLF institute in Amsterdam, in and around the 1980s. In both techniques one measures the scattered ion energies in specific directions (that define a scattering angle). These energies are determined by two factors, namely the recoil energy loss in the elastic binary collision with a near-surface atom and the inelastic loss (dominated by electronic excitation in MEIS) associated with the passage of the ion through the material. The recoil energy loss is characteristic of the mass ratio of the incident ion and scattering atom, while the inelastic loss is characteristic of the depth of the scatterer atom below the surface. Both methods thus provide depth-dependent compositional information by a method that is not (at least intrinsically) destructive. In MEIS the lower ion energies allow one to use dispersive electrostatic ion energy analysers that provide far higher spectral resolution that the solid-state detectors used in RBS. The lower energies also typically lead to higher rates of inelastic energy loss, so the combination of these two aspects provides substantially enhanced depth resolution.

For studies of surface structure one can exploit the narrow shadow cones associated with elastic scattering in the MEIS energy range. By using specific low index crystallographic incidence directions one can selectively (nominally) illuminate only one or two (or more) surface layers, and by studying the scattered yield as a function of scattering angle one can exploit the same elastic shadowing effects on the outward trajectory to determine the relative positions of surface and sub-surface atoms. The development of parallel detection analysers that simultaneously map the scattered signal over a range of scattered ion energies and angles [2] provide a means to measure these complete ‘blocking curves’ simultaneously.

One final important feature of the MEIS technique (also shared with RBS) is the ability to make absolute measurements of the scattered ion yield that can be related

directly to the number of surface and sub-surface layers contributing to a scattered ion signal.

While the MEIS technique was used extensively by the AMOLF Amsterdam group to investigate crystallographic effects at the surface and in near-surface interface formation, most of this work was focussed on semiconductor systems, and in recent years most MEIS instruments have been devoted to the study near-surface compositional variations in complex oxide films on silicon surfaces, motivated by the need to develop new high dielectric constant materials for the next generation of more compact semiconductor devices. Following the commissioning of a UK national MEIS facility at Daresbury Laboratory in the late 1990s (e.g. [3]), however, there have been renewed efforts by some groups to exploit the ability of MEIS to investigate structural aspects of surfaces of a wider range of materials. In this brief review a few of these applications performed by our own group are described to illustrate this capability. Of course, there are many other methods of surface structure determination, particularly based on electron scattering (such as low energy electron diffraction – LEED [4] – and photoelectron diffraction [5]) and X-ray scattering [6]. One can also obtain surface structural information from low energy (~1-50 keV) ion scattering, a method that is far more intrinsically surface specific due to the wider elastic shadow cones and a higher probability of charge transfer at the surface [7, 8], but this brief review focuses on the MEIS technique with examples that exploit its particular strengths of subsurface penetration, narrow shadow cones, extreme depth resolution, elemental specificity and absolute intensity calibration.

2. Alloy surfaces

One application that rather directly exploits the potential of MEIS to investigate the properties of discrete (small) numbers of outermost atomic layers of a crystalline surface is in the study of alloy surfaces. It is well-known that the thermodynamically favoured composition of the outermost few atomic layers of an alloy may differ from that of the bulk, but there are rather few methods available to obtain direct experimental information on this problem. MEIS does have this ability, as was first demonstrated in a study of $Pt_{50}Ni_{50}$(111) alloy surface [9] by the AMOLF group, and we have exploited this further in an investigation of $Pt_{25}Rh_{75}$(111) using 100 keV H^+

scattering [10]. Fig. 1 shows schematically the ion trajectories that can be used in MEIS experiments to extract the required compositional information. In particular, three different incident directions can be used to illuminate (nominally) the outermost one, two and three atomic layers. This suggests that from MEIS scattered ion energy spectra in these three directions one can determine the relative compositions of the outermost one, two and three layers and thus, by a simple solution of simultaneous equations, to determine the composition of each layer.

In reality, the situation is somewhat more complex. In a real solid the atoms are vibrating, so some of the incident ions will reach layers that are nominally shadowed according to the simple picture of Fig. 1, due to a surface atom being displaced from its equilibrium position at the moment that the ion passes. Static relaxations of the equilibrium positions of surface atoms from their ideal bulk-terminated locations will also lead to some sub-surface illumination. Clearly this partial illumination of additional layers leads to more complex simultaneous equations to solve, and it is important to know exactly what fraction of these deeper layers is illuminated. The problem can be somewhat reduced by choosing detection directions that correspond to blocking of outgoing trajectories from the unwanted sub-surface layers, so both ingoing and outgoing trajectories are nominally highly selective, but this use of so-called double-alignment geometries does not wholly overcome the problem.

Fig. 2 shows the MEIS scattered ion signals from the Pt and Rh atoms as a function of scattering angle for the three incident geometries of fig.1. A clear illustration of the influence of thermal vibrations and possible surface relaxation is seen in the data recorded in the $[0\bar{0}1]$ incidence direction, as for the Rh scattering signal, in particular, there is a clear blocking dip at 90º scattering angle, corresponding to a [110] outgoing direction. If only the outermost atomic layer was illuminated by incident ions there could be no blocking dip, because there would be no atoms between the outermost layer and the detector to produce the blocking. Evidently, there is some illumination of the second layer in this incidence direction, and we may infer from the relative absence of a blocking dip in the Pt signal that the visible Pt atoms are almost entirely in the outermost layer. Indeed, even in the [110] blocking dip the scattered ion signal corresponds to about 1.3 layers (0.8 layers Rh and 0.5 layers Pt), so some second

layer scattering overcomes even the double alignment geometry. Fig. 2 also shows, however, that by conducting full simulations of the ion scattering for this system using the VEGAS computer program [11], including the effects of (optimised) vibrational amplitudes, and optimised values of the layer-dependent composition and geometry, a fully consistent description of the experimental data is possible. Specifically, the results yielded Pt concentrations in the outermost, second and third atomic layers of 47 ± 2%, 5 ± 2% and 25 ± 3% respectively. Notice that the concentration in the third layer is already that of the underlying bulk. The simulations also provided information on the surface relaxations, indicating that in the outermost layer the Pt atoms are relaxed outwards from the bulk relative to the Rh atoms.

3. TiO_2(110) surface geometry

An example of an application of MEIS more specifically concerned with the determination of surface crystallography is provided by a recent study of the (rutile) TiO_2(110) clean surface [12]. While the surface relaxations and reconstructions of metal and semiconductor surfaces have been widely investigated by a range of methods, comparable information on oxide surfaces is sparse, despite the known importance of the surfaces of these materials. TiO_2 is perhaps the most widely studied material in surface science, in part because good single crystals are readily available and modest heating leads to the formation of bulk colour centres (O vacancies and/or Ti interstitials) that render the crystals conducting, avoiding the problem of surface charging when studied with ions or electrons. The detailed relaxations of the TiO_2(110) surface have nevertheless proved controversial [13], with many theoretical total energy calculations giving widely different values for the outermost several Ti and O atomic layers, and the only experimental study until recently, based on surface X-ray diffraction (SXRD), being inconsistent with most of these calculations.

To address this problem, 100 keV H^+ MEIS studies were recently conducted on this surface. The basic methodology was to measure a range of blocking curves (using four different incident directions chosen to give nominal one- and two-layer illumination) and to compare the experimental data with the results of VEGAS simulations for a range of trial structures. The quality of fit between theory and

experiment was assessed with the help of an *R*-factor (reliability-factor) based on a normalised mean-square-deviation of all the experimental and theoretically computed data points. A key problem in determining the detailed structure of this surface is the large number of potentially relevant structural parameters. While particular attention has been focussed on the relaxation of the four distinct outermost layer atoms in this surface (identified in fig. 3), earlier studies have provided evidence for significant relaxations of atoms as deep as the fourth or fifth layers, mainly perpendicular to the surface, but in some cases also parallel to the surface. For this reason, comparisons were first made of the MEIS experimental blocking curves with the results of VEGAS calculations for previously-identified structural models, two from earlier experiments (the early SXRD study [14] and a much more recent low energy electron diffraction (LEED) study [15]), and two from relatively recent theoretical total energy calculations [16].

These initial comparisons led to the conclusion that the structural model based on the recent experimental LEED investigation gave the best fit to the MEIS experiments, but these comparisons also showed that certain features in the blocking curves could be largely attributed to movements of specific near-surface atoms. In view of this a modified version of the simulation software was developed to provide an automated search of the rich parameter space to determine the structural parameter values giving the best fit to the MEIS data (fig. 4). Comparison of these parameter values with those of the earlier studies confirms the closest agreement with the LEED results, also broadly consistent with some related calculations, although some significant differences do remain. Perhaps most significantly, the MEIS results clearly show that the bridging oxygen atoms (fig. 3) are relaxed outwards from the surface, a result consistent with other more recent studies, but in sharp contrast to the strong inward relaxation reported on the basis of the earlier SXRD investigation. This is almost certainly the most challenging application so far of the MEIS technique in surface crystallography, and it is particularly noteworthy that the results proved quite sensitive in appropriate scattering geometries to the location of the weakly-scattering surface oxygen atoms.

4. Adsorbate-induced surface reconstructions

While early discussions of adsorption on surfaces tended to consider the substrate as a rigid atomic chequer-board on which the adsorbed atoms or molecules adopted well-defined adsorption sites, it has now long been recognised that adsorbates also lead to some modification of the structure of the outermost atomic layers of the underlying substrate. In some cases this effect is quite subtle, such as a small change in the outermost substrate layer spacing, or a small 'rumpling' of the first or second substrate layer due to differences in interlayer spacing of atoms covered or not covered by an adsorbed species [17]. In other cases, however, the changes to the underlying surface structure are more radical, with significant lateral movements of atoms parallel to the surface, or complete reorganisation to produce an outermost substrate layer with a different atomic concentration from that of the underlying bulk layers [17]. In some of these cases the reconstructed surface layer may only have rather long-range registry with the substrate (i.e. have a large surface unit mesh), or may even be incommensurate with the substrate, rendering most conventional methods of surface structure determination inapplicable or of limited value. In these cases MEIS has a particularly valuable role to play, because of its capacity to provide information on the number of displaced atoms in the surface through the combination of selected scattering geometries and appropriate absolute calibration of the scattering signal.

A particular illustration of this capacity arises from an interesting class of adsorbate-induced surface reconstructions, namely pseudo-(100) reconstructions of (especially) fcc (111) surfaces [18]. In this group of systems the hexagonal closed-packed outermost fcc(111) layer is replaced by a lower-density near-square array of substrate atoms on which the adsorbate occupies 4-fold coordinated hollow sites. The driving force for the reconstruction appears to be that the adsorption energy on a (100)-type surface is so much lower than on an unreconstructed (111) surface that the energy cost associated with the formation of the (111)/(100)-like interface can be accommodated. Of course, an ideal (100) layer on a (111) surface the structure would necessarily be incommensurate, due to the mismatch of the 4-fold and 3-fold rotational symmetries, but in practice some distortion of the nominally square symmetry of the reconstructed layer seems to occur to allow long-range commensuration. Until recently the evidence

for these reconstructions has been largely indirect, based on plausible interpretations of qualitative LEED patterns or on information regarding adsorbate-substrate interlayer spacings from normal-incidence X-ray standing wave (NIXSW) measurements that are most obviously compatible with such a model. More recently scanning tunnelling microscopy (STM) images provide direct evidence of the near-square symmetry of the surface layer, but still fail to establish directly the identity of the imaged atoms.

One example of this type of reconstruction is provided by the Cu(111)/CH_3S surface phase in which the methylthiolate adsorbate can be produce at the surface by exposure to methanethiol (CH_3SH) that deprotonates at the surface, or to dimethyldisulphide ($(CH_3S)_2$) which suffers S-S bond scission on the surface. This model adsorption system is of interest in the study of alkanethiol self-assembled monolayer (SAM) systems on coinage metal surfaces. The fact that this surface involves an adsorbate-induced density-lowering surface reconstruction was identified in early NIXSW and X-ray absorption experiments [19], but it is through more recent STM studies that the pseudo-(100) nature of the reconstruction was first implicated [20]. While exact commensuration is difficult to establish through STM, this study led to the suggestion that the structure could be described by a $\begin{bmatrix} 4 & 3 \\ -1 & 3 \end{bmatrix}$ commensurate unit mesh, implying the Cu atoms in the reconstructed layer are arranged on a near-rectangular mesh with dimensions 2.88 Å by 2.95 Å, almost 15% larger in both directions than the 2.55 Å square of the Cu(100) surface (fig. 4). From the point of view of a MEIS study there are two important implications of this description. First, the more open packing of a square mesh relative to a close-packed hexagonal one, combined with the slightly larger periodicity, means that the density of Cu atoms in a reconstructed layer contains only 0.66 ML of Cu atoms where 1 ML is the atom density in a Cu(111) layer. Secondly, the large commensurate mesh (or even incommensurate structure) means that (almost) all the Cu atoms in the reconstructed layer are displaced from bulk-continuation sites, and so will contribute little or no shadowing and blocking in a MEIS experiment. This means that a single layer reconstruction of this type may be expected to lead to an enhanced Cu scattering signal relative to the clean surface of

essentially this number of displaced Cu atoms. In the event that more than one Cu layer is reconstructed, further enhancement of the Cu scattering signal is anticipated.

Fig. 5 shows a subset of the data from the MEIS study of this system [21] in the form of blocking curves recorded in the nominal one-layer incident illumination direction of $[\bar{1}\bar{1}0]$. The experimental data points are compared with the results of VEGAS calculations for the clean surface, for the one-layer reconstruction model of fig. 4, and for an alternative model involving two such reconstructed Cu layers. Clearly the one-layer reconstruction model fits the experimental data well and provides direct confirmation of this structure. Notice, though, that the offset is the scattered ion signal between the data from the clean surface and from the thiolate overlayer does not differ by the 0.66 ML mentioned above, but by less than this amount. The reason for this is related to the role of surface layer atomic vibrations. On the clean Cu(111) surface (as on other metal surfaces), it is well established that the outermost layer atoms have significantly enhanced vibrational amplitudes relative to those of the underlying bulk, particularly perpendicular to the surface. These enhanced vibrational amplitudes lead to enhanced visibility of second (and lower) layer scattering contributions to the scattered ion signal, even in this nominal one-layer shadowing incident direction. Indeed, for this reason, even in the double-alignment blocking dips the scattered ion signal exceeds that expected from a single Cu(111) layer. However, when the thiolate adsorbate causes a reconstruction of this layer, the underlying outermost unreconstructed Cu(111) layer is no longer the surface layer, and no significant enhancement of the vibrational amplitudes of the atoms in this layer is to be expected. Thus, while the reconstruction leads to an extra 0.66 ML of scattering from the reconstructed layer, the scattered intensity from the underlying substrate is less than that of a clean surface. Notice, incidentally, that because the Cu atoms in the reconstructed layer are (statically) displaced from bulk continuation sites, any possible enhanced vibrational amplitude of these atoms has no impact on the detected scattered ion yield.

While this reconstruction clearly leads to an enhancement of the absolute scattering yield, the fact that an increased number of layers contribute to the scattering signal should also lead to a modification of the scattered ion energy spectrum in the Cu

scattering signal, because scattering from Cu layers further from the surface leads to increased inelastic energy loss. As shown in fig. 6, this is, indeed, the case; the 'surface peak' from scattering from the Cu atoms in the $[\bar{1}\bar{1}0]$-incidence, [001]-exit double-alignment geometry is wider as well as having a larger area. Fig. 6 shows that this effect can be simulated in a rather simplistic fashion. To do this, the shape of the energy-loss spectrum from a single layer (including instrumental broadening), modelled by an asymmetric Gaussian, was first optimised by fitting to the experimental clean surface spectrum, using the VEGAS calculations to determine the relative intensity of scattering from each of the outermost layers, and offsetting these layer contributions by the energy loss given by the SRIM code [22]. The same layer energy loss offsets were then inserted into a simulation of reconstructed surface, again using the VEGAS calculations to determine the relative intensity of scattering from each of the outermost layers. This procedure, first developed in a study of the Cu(111)/N pseudo-(100) reconstruction adsorbate system [23], proved particularly valuable in that case due to the influence of subsurface damage associated with the low energy N-ion implantation used prior to annealing to form the N chemisorption phase, but also provides useful confirmation of the methylthiolate reconstruction model.

Very recently a similar procedure has been used in a MEIS study [24] of the methylthiolate-induced reconstruction of Ag(111), in this case to form a much simpler ($\sqrt{7}$x$\sqrt{7}$)R19° surface phase. This structure is not thought to involve a pseudo-(100) reconstruction, but rather a reconstructed layer of Ag of hexagonal symmetry similar to that in Ag_2S(111), with a coverage of only 3/7 ML. Here too MEIS provides clear support for this model that had previously only been inferred indirectly from STM [25] and NIXSW [26] studies.

5. Conclusions

These few examples of more recent applications of MEIS to surface structure determination highlight the capability of the technique to investigate quite a wide range of materials (metals and oxides as well as semiconductors) and surface phenomena, including segregation, relaxation and reconstruction, and in particular to

gain information not readily obtained by other methods. So far most of these applications exploit the use of blocking curves with carefully calibrated absolute yields and associated simulations based on the original VEGAS computer code.

The addition of simulations of scattered ion energy spectra highlight the monolayer resolution of the MEIS technique, and while such methods are widely used in depth-profiling of thin films, it seems they could play an important role in further developments of MEIS for surface structure determination. However, at least in the simple form illustrated here, considerable caution may be required. The SRIM code takes no account of the crystalline character of the sample and thus provides an averaged energy loss per layer traversed by the ions. In reality, however, the energy loss will be trajectory dependent, larger energy losses resulting from trajectories that pass very close to atoms, such as those reaching second-layer atoms in a nominal one-layer shadowing or blocking geometry. Progress is now being made in proper treatment of the details of the energy losses and their trajectory dependence [27, 28], and it remains to be seen how fruitful this will prove in putting this extension of the current methodology on a firmer footing.

Acknowledgements

The author is happy to acknowledge the crucial role paid by many collaborators (as cited in the various publications), both at Warwick and at Daresbury Laboratory, in making possible the work reported here. The funding support of the Engineering and Physical Sciences Research Council (UK) is also gratefully acknowledged.

Figure Captions

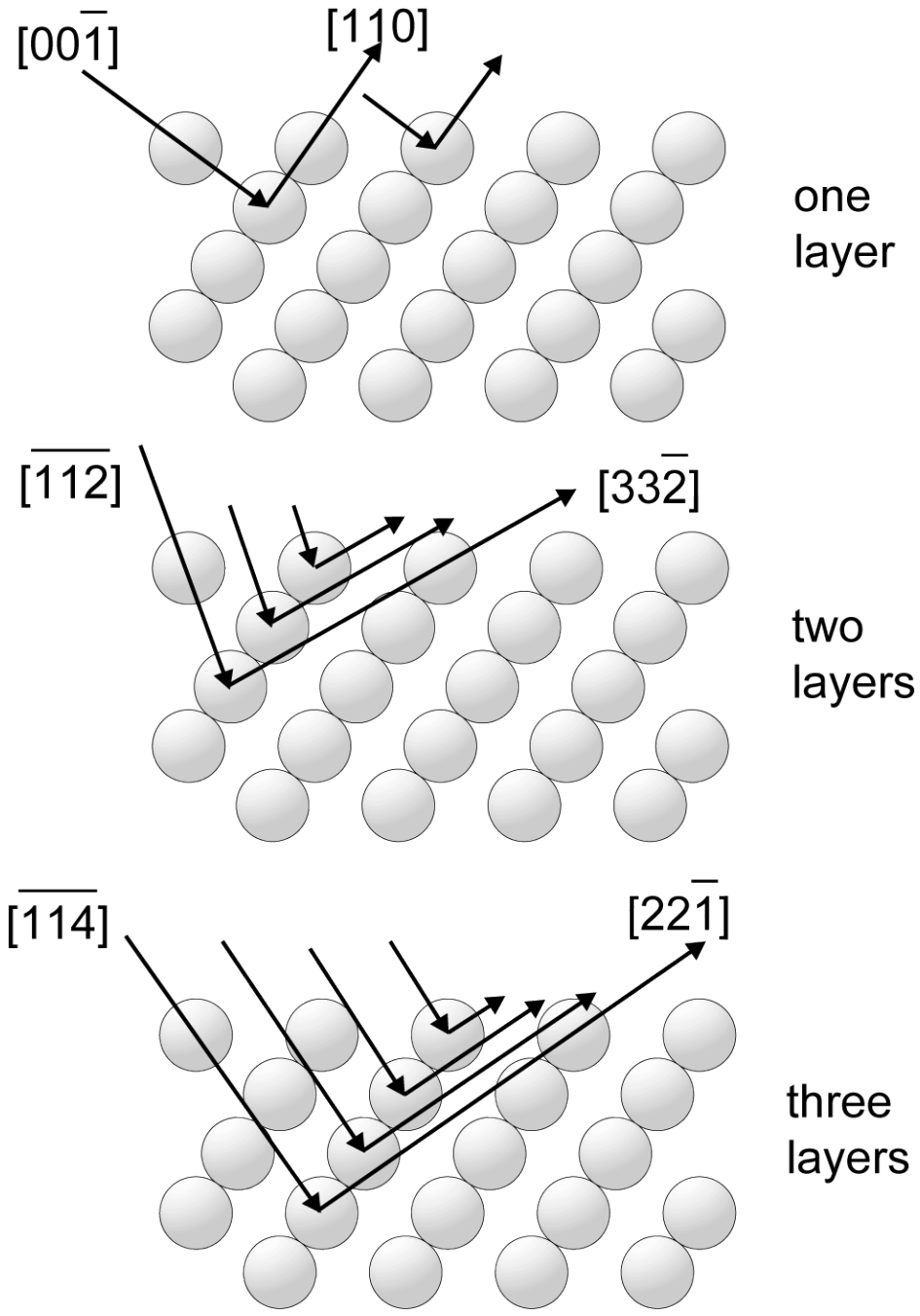

Fig. 1. Schematic diagram of a side view of an fcc (111) surface in a <112> azimuth showing three different ion incident directions that illuminate discrete numbers of surface layers in an ideally-terminated bulk solid. Also shown are double-alignment detection directions that enhance this layer selectivity.

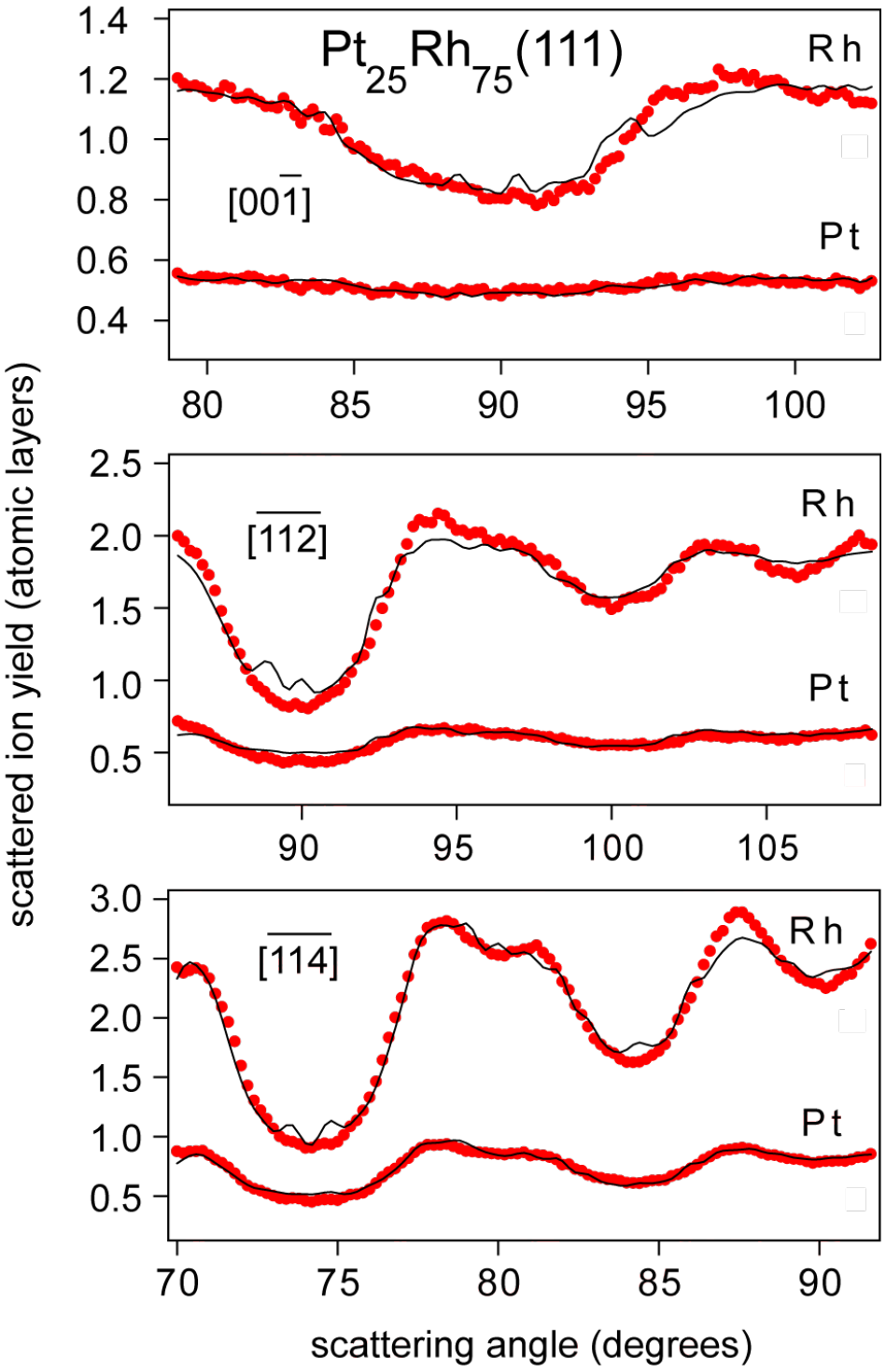

Fig. 2 MEIS blocking curves for the Rh and Pt scattering signals from $Pt_{25}Rh_{75}(111)$ after annealing to 900 K recorded in three different incident directions chosen to nominally illuminate the outermost one, two and three atomic layers as shown in fig. 1. The experimental data are shown by individual data points, the theory by continuous lines. After ref. [10]

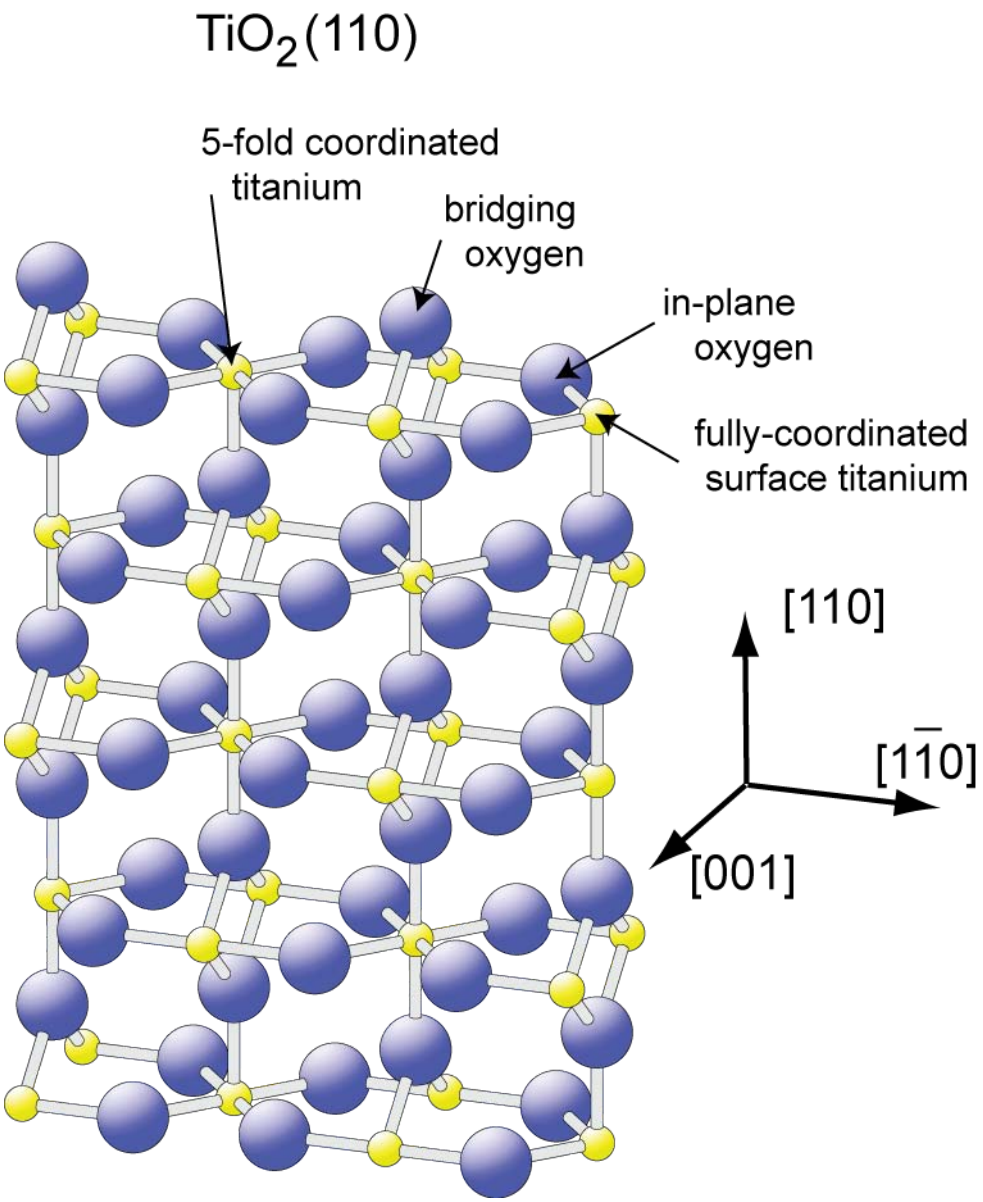

Fig. 3 Schematic diagram of the TiO_2(110) surface with the outermost layer Ti and O atoms labelled.

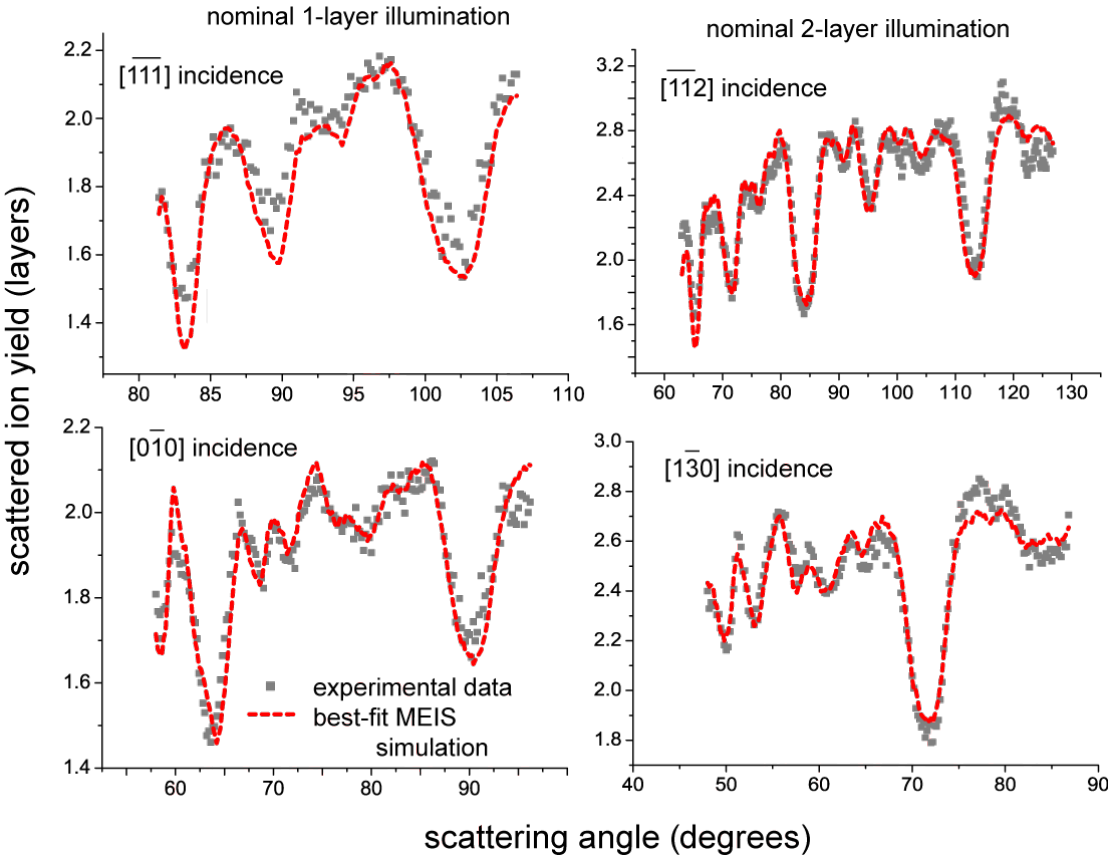

Fig. 4. Comparison of experimental 100 keV H^+ MEIS blocking curves from a TiO_2(110) surface in four different incident directions with the results of simulations for the best-fit structural model

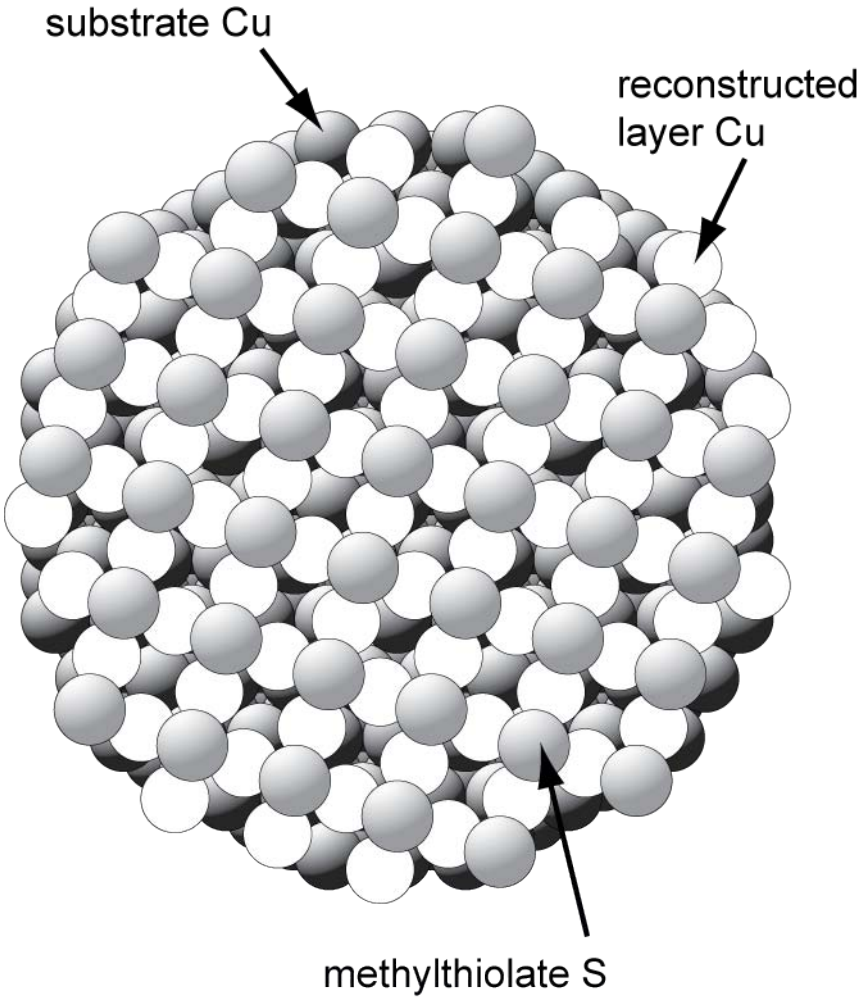

Fig. 5 Schematic plan view of the proposed structure of the reconstructed Cu(111)/CH_3S surface.

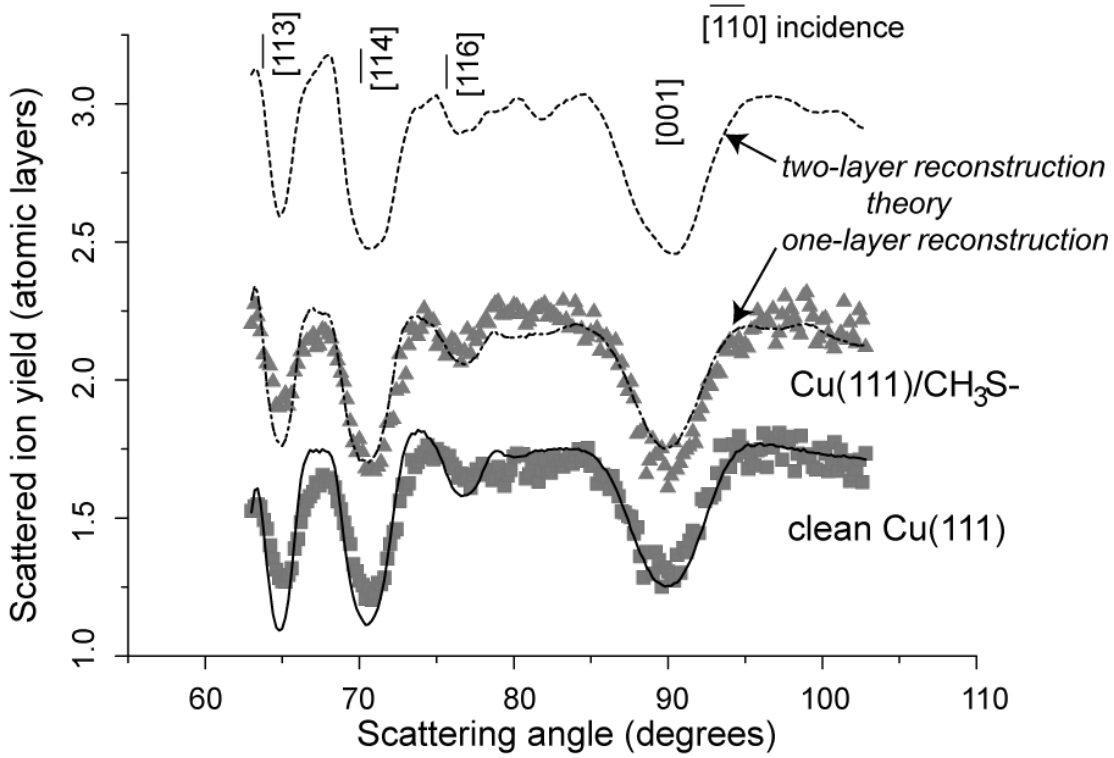

Fig. 6 100 kev H^+ MEIS blocking curves of the Cu scattering signal recorded in [$\bar{1}\bar{1}$0] incidence from clean Cu(111) and from the same surface after the formation of the methylthiolate overlayer structure. The experimental results are shown as individual data points while the continuous lines are the results of VEGAS simulations.

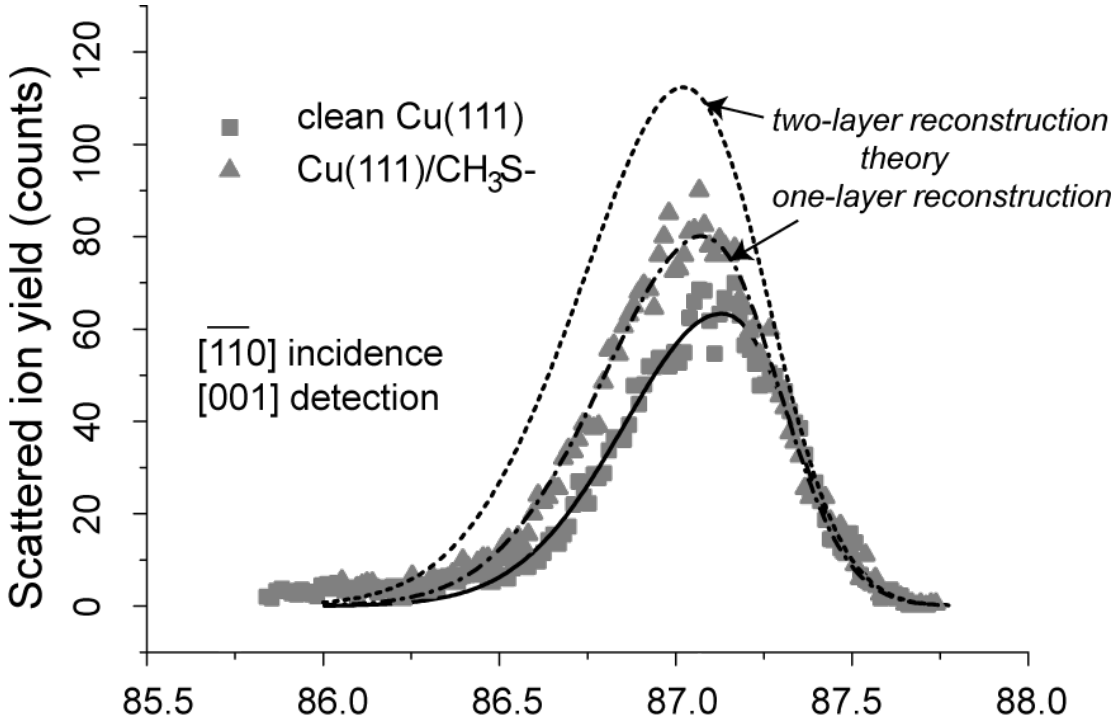

Fig. 7. 100 kev H^+ MEIS scattered ion energy spectra of the Cu scattering signal recorded in the double-alignment geometry of [$\bar{1}\bar{1}$0] incidence and [001] detection from clean Cu(111), and from the same surface after the formation of the methylthiolate overlayer structure. The experimental results are shown as individual data points while the continuous lines are the results of simulations as described in the text.

References

1 J.F. van der Veen, Surf. Sci. Rep. 5 (1985) 199

2 R.M. Tromp, M. Copel, M.C. Reuter, M. Horn von Hoegen, J. Speidell and R. Koudijs, Rev. Sci. Instrum. 62 2679 (1991)

3 P.Bailey, T.C.Q. Noakes and D.P. Woodruff, Surf. Sci. 426 358 (1999)

4 K. Heinz Rep. Prog. Phys. 58 (1995) 637

5 D. P. Woodruff, A..M. Bradshaw Rep. Prog. Phys. 57 (1994) 1029

6 I. K. Robinson, D.J. Tweet Rep. Prog. Phys. 55 (1992) 599

7 H. Niehus, W. Heiland, E. Taglauer, Surf. Sci. Rep.17 (1993) 213

8 J. W. Rabalais, *Principles and Applications of Ion Scattering Spectrometry: Surface Chemical and Structural Analaysis* (J. Wiley, New York, 2002)

9 S. Deckers, F.H.P.M. Habraken, W.F. van der Weg, A.W. Denier van der Gon, B. Pluis, J.F. van der Veen, R. Baudoing, Phys. Rev. B 42 (1990) 3253

10 D. Brown, P.D. Quinn, D. P. Woodruff, T.C.Q Noakes, P. Bailey, Surf. Sci. 497 (2002) 1

11 R.M. Tromp and J.F. van der Veen, Surf. Sci. 133 (1983) 159

12 G. S. Parkinson, M. A. Muñoz-Márquez, P. D. Quinn, M. J. Gladys, R. E. Tanner, D. P. Woodruff, P. Bailey, T. C. Q. Noakes, Phys. Rev. B 73 (2006) 245409

13 U. Diebold, Surf. Sci. Rep. 48 (2003) 53

14 G. Charlton, P. B. Howes, C. L. Nicklin, P. Steadman, J. S. G. Taylor, C. A. Muryn, S. P. Harte, J. Mercer, R. McGrath, D. Norman, T. S. Turner, G. Thornton, Phys. Rev. Lett. 78 (1997) 495

15 R. Lindsay, A. Wander, A. Ernst, B. Montanari, G. Thornton, N..M. Harrison, Phys. Rev. Lett. 94 (2005) 246102

16 V. Swamy, J. Muscat, J. D. Gale, N. M. Harrison, Surf. Sci. 504 (2002) 115

17 D. A. King, D. P. Woodruff , eds. *Phase Transitions and Adsorbate Restructuring at Metal Surfaces : The Chemical Physics of Solid Surfaces, volume 7* (Elsevier, Amsterdam, 1994)

18 D. P. Woodruff, J.Phys.:Condens.Matter 6 (1994) 6067

19 N.P.Prince, D.L.Seymour, D.P.Woodruff, R.G.Jones and W.Walter, Surf. Sci. 215 (1989) 566

20 S.M.Driver and D.P.Woodruff**,** Surf. Sci. 457 (2000) 11

21 G. S. Parkinson, M. A. Muñoz-Márquez, P. D. Quinn, M. Gladys, D. P. Woodruff, P. Bailey, T. C. Q. Noakes, Surf. Sci. 598 (2005) 209

22 J.F. Ziegler, SRIM code, http://www.SRIM.org

23 M.A. Muñoz-Márquez, G. Parkinson, P.D. Quinn, M. Gladys, R.E. Tanner, D.P. Woodruff, T.C.Q.Noakes and P.Bailey, Surf. Sci. 582 (2005) 97

24 G. S. Parkinson, A. Hentz, P. D. Quinn, A. J. Window, D. P. Woodruff, P. Bailey, T. C. Q. Noakes, Surf. Sci. submitted for publication

25 Miao Yu, S.M. Driver and D.P. Woodruff, Langmuir 21 (2005) 7285

26 Miao Yu, D.P.Woodruff, N. Bovet, C.J. Satterley, K. Lovelock, Robert G. Jones, V. Dhanak, J. Phys. Chem. B 110 (2006) 2164

27 P.L. Grande, A. Hentz, G. Schiwietz, W.H. Schulte, B.W. Busch, D. Starodub, and T. Gustafsson, Phys. Rev. B 69 (2004) 104112

28 M.A. Muñoz-Márquez, G.S. Parkinson, D.P. Woodruff, A. Hentz, P.L. Grande, G. Schiwietz, T.J. Wood, C. Bonet, S.P. Tear, P. Bailey, T.C.Q. Noakes, Phys. Rev. B, 72 (2005) 075415